Thermal Performance Enhancement of Double-Slope Solar Still Using Phase Change Material: Numerical Investigation and Energy Analysis under Casablanca Climatic Conditions.

Asmaa Ait Baha[1*], *Wissal* Nahairy[1] Naoual, Belouaggadia[1], Omar Bouattane[2], Abdellah Zamma[1].

[1] *Laboratory of Modeling and Simulation of Intelligent Industrial Systems (M2S2I), ENSET Mohammadia, Hassan II University of Casablanca, Morocco.*
[2] *Electrical Engineering and Intelligent Systems (IESI), ENSET Mohammadia, Hassan II University of Casablanca, Morocco.*

Abstract. This study presents a comprehensive numerical investigation of a double-slope solar still integrated with phase change material (PCM) under the Mediterranean climate of Casablanca. A five-node transient thermal model was developed using Python, incorporating detailed geometrical parameters (1.0 m² basin area, 0.05 m water depth, 0.02 m PCM thickness, 33° glass inclination) and validated heat transfer correlations. The model simulated 24-hour operation for both conventional and PCM-enhanced configurations using meteorological data from peak solar intensity days.

Results demonstrate that paraffin wax PCM (melting point 60°C) effectively regulates thermal dynamics, reducing peak water temperature by 13°C from 89°C to 76°C while maintaining operational stability. The PCM exhibited a 14-hour phase transition cycle, enabling significant thermal energy time-shifting that increased overall daily productivity by 10.5% from 3.8 to 4.2 kg/m². Most notably, nocturnal distillate yield increased by 180%, extending productive operation from 12 to 18 hours daily and shifting 28% of total evaporative energy to post-sunset periods compared to only 8% in conventional operation.

The study provides validated evidence that simple PCM integration transforms solar stills from intermittent to continuous producers, offering enhanced reliability for remote applications. The computational framework establishes a robust foundation for optimizing PCM-based thermal storage in solar desalination systems, demonstrating practical pathways for performance improvement without mechanical complexity.

*Corresponding author: asmaa.aitbaha1994@gmail.com

1. Introduction:

Water scarcity is a growing Global issue affecting billions of people, particularly in arid and semi-arid regions where natural freshwater resources are insufficient. According to the United Nations, more than two-thirds of the world's population could face water shortages by 2040 if current trends continue. Conventional water supply methods, such as groundwater pumping or large-scale transfers, are increasingly unsustainable due to overexploitation, pollution, and climate change. Consequently, desalination of saline and brackish water has become an essential alternative for securing potable water in water-stressed regions.[1], [2] Several desalination technologies are available, including thermal processes such as multi-stage flash (MSF) and multi-effect distillation (MED), as well as membrane-based processes like reverse osmosis (RO) and electro dialysis (ED). While these technologies are effective on an industrial scale, they are highly energy-intensive, require sophisticated infrastructure, and generate concentrated brine that can harm the environment. Their deployment in rural or off-grid areas is often unfeasible due to their dependence on fossil fuels and high capital costs. This limitation has stimulated interest in solar desalination, which directly harnesses renewable solar energy[3], [4], [5]. Solar desalination offers an environmentally sustainable solution by using solar radiation either to generate electricity that powers conventional desalination units or to heat water in thermal processes directly[6]. Direct solar desalination systems, such as solar stills[7], are often required in remote locations due to their simplicity, low cost, and independence from external energy sources.
Solar distillers function as a controlled representation of the natural hydrological cycle. In this process, solar radiation drives the evaporation of saline or impure water contained in the basin, and the resulting vapor condenses on the inner surface of a transparent cover, thereby generating distilled water analogous to precipitation.[8]

As illustrated in Figure 1, they can be classified according to different criteria. Based on the energy source, they are divided into passive and active systems. Passive solar stills rely exclusively on direct solar radiation for heating and evaporation, making them simple in design, low in cost, and free of mechanical components. In contrast, active solar stills incorporate external devices, such as solar collectors, photovoltaic panels, heat exchangers, or heat pipes, to enhance evaporation, thereby increasing efficiency at the expense of higher complexity and cost. A second classification is related to the geometrical configuration, which includes single-slope and double-slope basin stills as the most common types, alongside alternative designs such as pyramid-shaped, conical, and tubular stills, each intended to improve condensation and freshwater yield. Finally, solar stills can also be categorized by the basin arrangement: single-effect systems operate with a single evaporation–condensation cycle, multi-effect basins employ multiple sequential stages to maximize productivity, and stepped or cascaded basins allow water to flow over successive levels, thereby enlarging the evaporation surface and improving distillate output.[8], [9].

The geometry of the still has a substantial impact on performance. Single-slope and double-slope basin stills are the most widely studied and implemented due to their ease of construction and low cost.[10] However, their output is limited, typically ranging from 2 to 5 L/m²/day, depending on climatic conditions [11]. Numerous geometrical variations have been investigated to overcome these limitations, including stepped designs, wick-type basins, finned and corrugated absorbers, hemispherical and pyramid-shaped covers, as well as rotating-drum and tubular configurations.[12], [13], [14].

Recent bibliometric analyses have highlighted a growing research focus on solar stills integrated with phase change materials (PCMs) as an emerging solution to water scarcity in arid regions.as shown in figure 2, Between 2015 and 2025, publications increasingly linked solar stills*,* solar heating*,* phase change materials*, and* heat storage *with keywords such as* productivity*,* thermal performance*, and* paraffin, reflecting a strong trend toward enhancing energy-storage-based desalination. Studies evolved from traditional distillation concepts toward hybrid systems combining thermal energy storage**,** nanoparticle-enhanced PCMs**,** and economic performance assessments. This shift indicates a clear scientific consensus that coupling solar distillation with latent-heat materials substantially improves efficiency and reliability, forming the foundation for the present numerical investigation on PCM-assisted solar stills under Casablanca climatic conditions[15][16].

Despite decades of research, the primary drawback of solar stills remains their low productivity and discontinuous operation, which is restricted to daylight hours. To enhance performance, researchers have proposed two broad approaches: design improvements, such as optimizing basin depth, inclination, and materials, or integrating fins, wicks, and reflectors;[17], [18], [19], [20] and operational improvements, such as coupling with external solar collectors, using nano-fluids, or applying external condensers. Reported enhancements range from 20% to over 70% compared to conventional single-basin designs[21], [22], [23], [24]. Nevertheless, the intermittent nature of solar energy continues to limit daily output, particularly in the evenings and at night, when demand for drinking water persists. Phase Change Materials (PCMs) have been introduced as a promising solution to address the issue of discontinuous freshwater production. PCMs store thermal energy in the form of latent heat during melting and release it during solidification, thereby acting as a thermal buffer. Their integration into solar stills allows extended operation after sunset and smoother thermal performance, resulting in higher cumulative yield[25][15].

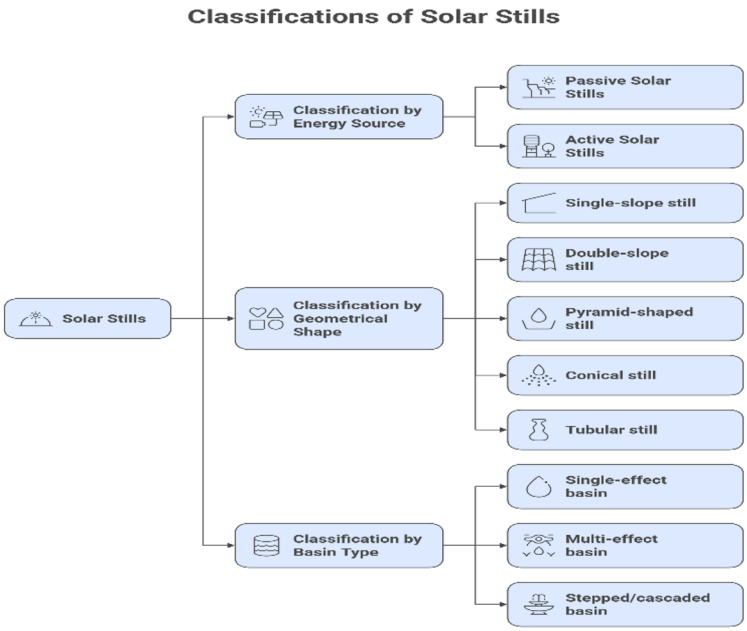

Figure 1: Classification of solar still in the Literature

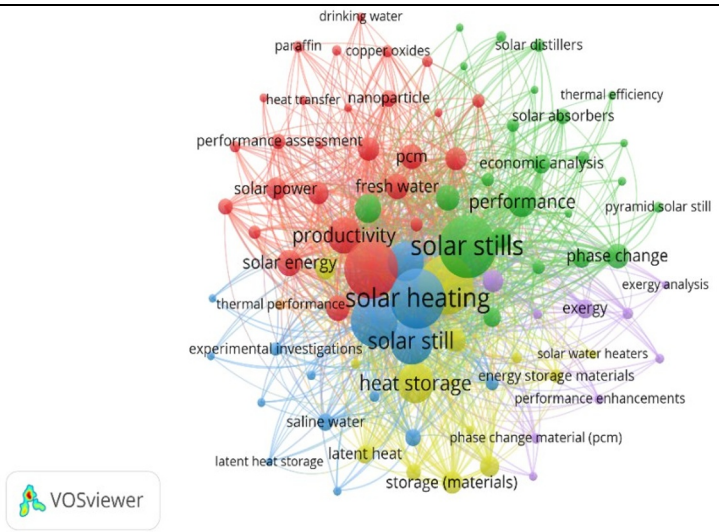

Figure 2 : the keywords map of solar stills and phase change materials co-occurrence (2015-2025)

PCMs are classified into three main categories: organic (e.g., paraffin wax, fatty acids), inorganic (e.g., salt hydrates), and eutectic mixtures. For solar still applications, organic PCMs such as paraffin wax are most commonly used due to their melting point range (40–60 °C), chemical stability, availability, and safety. Paraffin-based PCMs have demonstrated significant improvements in freshwater [26][27].In this context, the present study focuses on the thermal modeling of a double-slope solar still integrated with PCM under Casablanca climatic conditions. A nodal numerical model is developed to simulate transient heat and mass transfer mechanisms, including conduction, convection, radiation, and phase change. The aim is to analyze the thermal response of the system, highlight the role of PCM in stabilizing and extending freshwater production, and provide a methodological foundation for future experimental validation.

2. Methodology:

2.1 Geometric and physical properties of Materials:

The system under study is a double-slope solar still equipped with a 2 cm paraffin wax PCM layer beneath a 1 m × 1 m galvanized iron basin. A 3 cm glass-wool insulation layer minimizes heat losses, while two 4 mm glass covers inclined at 33° enable condensation and distillate collection on both sides.The system operates under Casablanca climatic conditions, using hourly data of solar radiation, ambient temperature, and wind speed. Its thermal behavior is represented by a five-node transient model (water, basin, PCM, and east/west glass covers) solved numerically over 24 hours using the Runge–Kutta (RK45) method.

All geometric, optical, and thermal properties of the materials used in the simulation are detailed in Tables 1 and 2.

Table 1: geometric properties

Description	***Value***
Basin length	1.0m
Basin width	1.0m
Basin height	0.10m
Water depth in the basin	0.05m
Vertical distance between the water surface and the glass	0.10m
Glass inclination (from horizontal)	33°
Glass thickness	0.004m
Water surface area (L×WL \times W)	1.0m²
Inner glass area (in contact with vapor)	1.0 m²
Basin surface in contact with water	1.0 m²

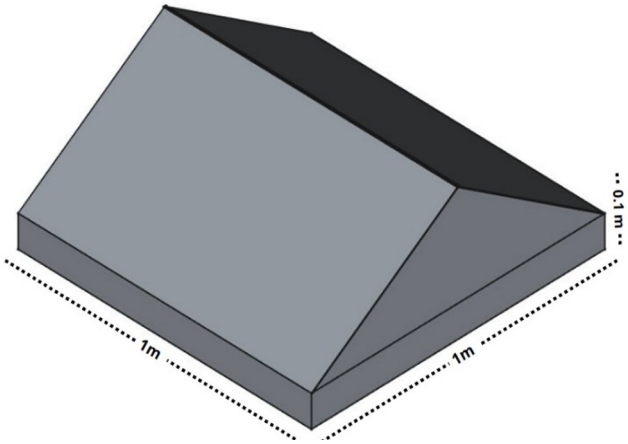

Figure 3 : double slope solar still geometry dimensions

)

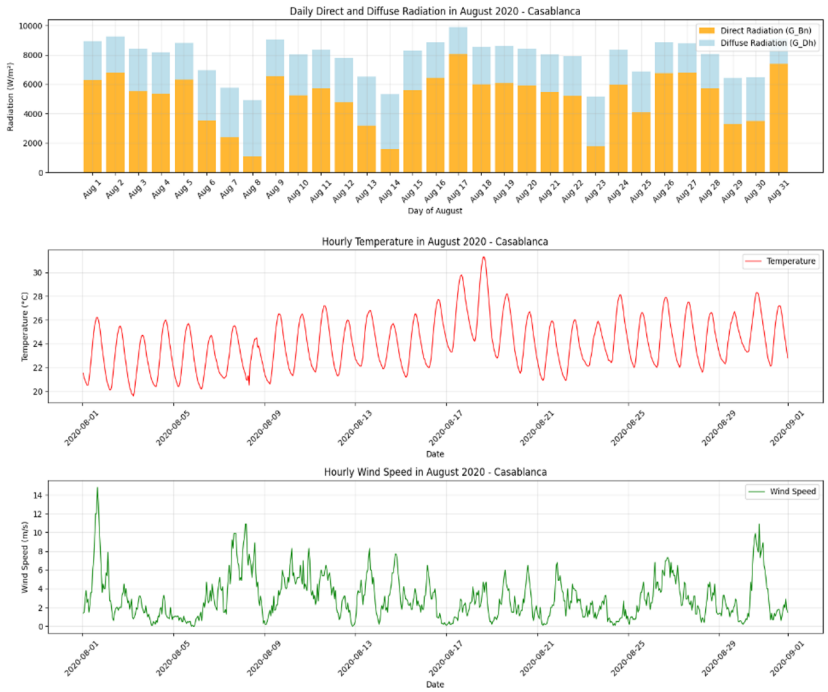

Figure 4 :Climatic parameters of Casablanca in 2020 (from meteonorm database)

Table 2 : properties of paraffin wax in the literature

Property	***Symbol***	***Value***
Melting temperature	Tm	56 °C
Latent heat of fusion	L	160 kJ/kg
Thermal conductivity	k	0.2 W/m·K
Density (solid)	ρs	880 kg/m³
Density (liquid)	ρl	770 kg/m³
Specific heat capacity	cp	2.0 kJ/kg·K

The simulation utilized hourly climatic parameters representative of Casablanca (33.6°N, 7.6°W) for a typical clear-sky summer day. Solar irradiance, ambient air temperature, and wind speed in figure 4 were imported from *Meteonorm* database and used as time-dependent boundary conditions in the model. These variables directly affect the solar input to the basin, the convective coefficients over the glass cover, and the overall heat-loss rate of the system. Their integration allows a realistic estimation of the still's transient thermal behavior under local operating conditions.

2.2 Assumptions:

The numerical model of the double-slope solar still with PCM is developed under the following assumptions, consistent with those commonly adopted in the literature (Tiwari & Kumar 2017)[28]

- All heat transfer processes are one-dimensional and uniform over each surface.
- Thermophysical and optical properties of materials are constant, except for the PCM, where the adequate specific heat varies within the melting range.
- The water layer is perfectly mixed, having a uniform temperature.
- Sidewall losses are neglected; only top and bottom heat losses are considered.
- The radiative exchange between water and glass is treated using an equivalent emissivity.
- The PCM (paraffin wax) melts and solidifies uniformly between 58 °C and 62 °C.
- Condensate removal does not affect the thermal balance of the system.
- The system is modeled for transient operation using hourly climatic data of Casablanca (solar irradiance, ambient temperature, wind velocity).

2.3 Governing Energy Balance Equations:

(1) Energy balance for the water layer

$$m_w c_w \frac{dT_w}{dt} = \alpha_w I A_b + h_{bw} A_b (T_b - T_w) - A_g \left[(h_c + h_e + h_r)_e (T_w - T_{ge}) + (h_c + h_e + h_r)_w (T_w - T_{gw}) \right] \quad (1)$$

(2) Energy balance for the glass cover

$$m_g c_g \frac{dT_g}{dt} = \alpha_g I A_g + A_g(h_c + h_e + h_r)(T_w - T_g) - A_g\left[h_w(T_g - T_a) + h_{r,sky}(T_g - T_{sky})\right] \quad (2)$$

(3) Energy balance for the basin liner

$$m_b c_b \frac{dT_b}{dt} = \alpha_b I A_b - h_{bw} A_b (T_b - T_w) - h_{bp} A_b (T_b - T_{pcm}) \quad (3)$$

(4) Energy balance for the PCM layer

$$m_{pcm} c_{pcm,eff} \frac{dT_{pcm}}{dt} = h_{bp} A_b (T_b - T_{pcm}) - U_{bot} A_b (T_{pcm} - T_a) \quad (4)$$

Where :

A_b – basin area (m²)

A_g – glass cover area (m²)

T_w – water temperature (°C)

T_b – basin liner temperature (°C)

Tg – glass cover temperature (°C)

T_{pcm} – PCM temperature (°C)

Ta – ambient air temperature (°C)

Tsky – effective sky temperature (°C)

mw, mb, mg, m_{pcm} – mass of water, basin, glass, and PCM (kg)

cw, cb, cg, $c_{pcm,eff}$ – specific heat of water, basin, glass, and PCM ($J \cdot kg^{-1} \cdot K^{-1}$)

I – incident solar irradiance ($W \cdot m^{-2}$)

αw, αb, αg– absorptance of water, basin, and glass (–)

h_{bw}– heat-transfer coefficient between basin and water ($W \cdot m^{-2} \cdot K^{-1}$)

hbp– heat-transfer coefficient between basin and PCM ($W \cdot m^{-2} \cdot K^{-1}$)

hc, he, hr) – convective, evaporative, and radiative coefficients ($W \cdot m^{-2} \cdot K^{-1}$)

hw – convective coefficient between glass and ambient air ($W \cdot m^{-2} \cdot K^{-1}$)

$h_{r,sky}$ – radiative coefficient between glass and sky ($W \cdot m^{-2} \cdot K^{-1}$)

2.4 Climate integration:

Figure 5 illustrates the solar radiation profile for August 17, showing a characteristic bell-shaped curve that peaks at approximately 950 W/m² around midday, delivering a total integrated daily energy of 6.8 kWh/m². *Figure 6* presents the corresponding ambient temperature trend, which lags the solar peak by several hours, reaching a maximum of 32°C in the mid-afternoon and maintaining relatively warm nocturnal temperatures above 24°C. *Figure 7* displays the wind speed pattern, which increases gradually throughout the

day to a late afternoon maximum of 4.8 m/s, providing enhanced convective cooling during critical condensation periods. Together, these figures characterize the synergistic climatic conditions—intense solar input, moderated thermal environment, and favorable wind patterns—that collectively enable the PCM to effectively store excess daytime energy and release it during extended nocturnal operation, thereby facilitating the observed 180% increase in nighttime productivity.

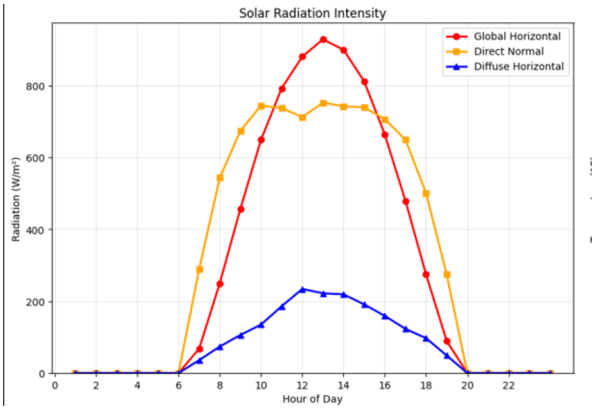

Figure 7: solar radiation over 24 of the day 17-08

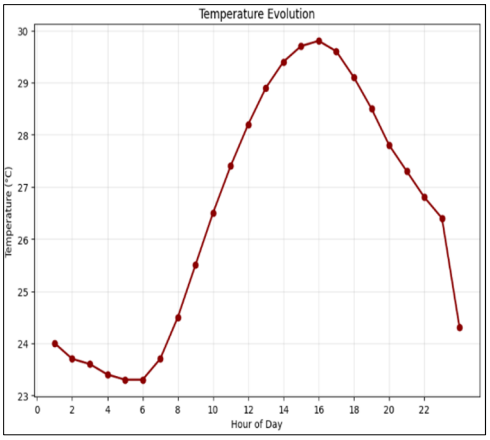

Figure 6: temperature of the air over 24h of 17-08

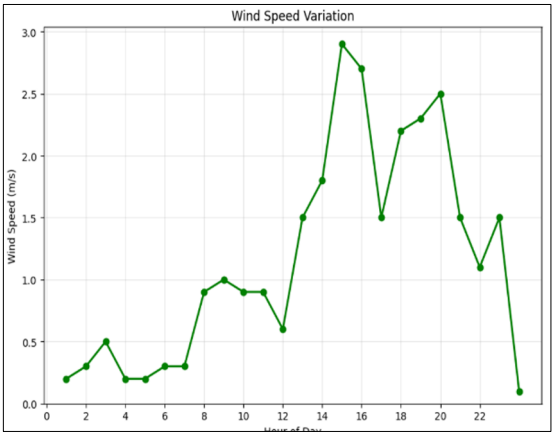

Figure 5: wind speed over 24h of the day 17-08

2.5 Numerical Implementation

The transient heat-transfer model of the double-slope solar still with PCM was solved in Python using the `solve_ivp` function from *SciPy* with the adaptive Runge–Kutta (RK45) method. The system was represented by five thermal nodes—water, basin, PCM, and east and west glass covers—each governed by a first-order energy balance equation. Hourly climatic data for Casablanca served as boundary conditions, while the thermal and optical properties of materials were taken from Tables 1 and 2. At each time step, the solver updated node temperatures based on instantaneous solar input and heat exchanges by convection, radiation, and conduction. The resulting temperature evolution was used to compute

evaporative fluxes and hourly distillate yield. Outputs were stored and visualized with *Matplotlib* to compare system performance with and without PCM.

3. Results and discussion:

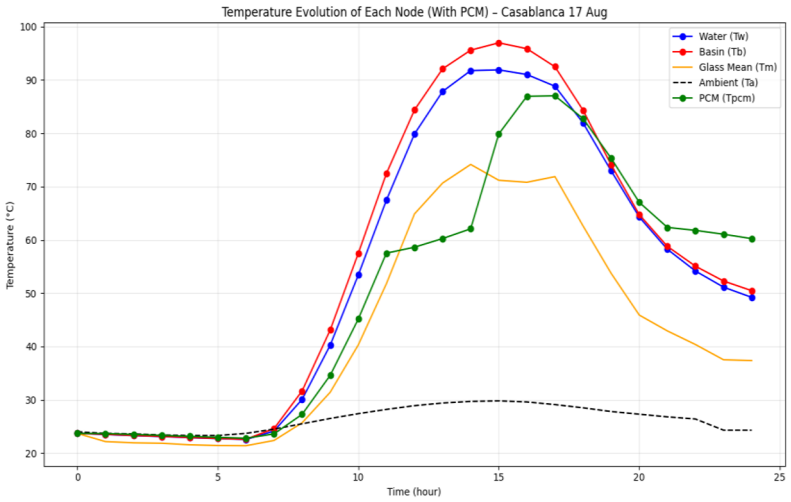

Figure 8 : temperature evolution of each node over 24h

The thermal behavior across the five system nodes in *figure 8* reveals distinct phase-dependent characteristics that validate the PCM's thermal regulation function. During daylight hours (6h-18h), the basin temperature exhibits the most rapid response to solar irradiation, consistently maintaining the highest temperature due to direct radiation absorption. The water temperature follows closely but demonstrates a moderated thermal profile, particularly in the PCM-equipped configuration where peak temperatures are reduced by approximately 10-15°C compared to the non-PCM case. This attenuation represents the PCM's primary function: absorbing excess thermal energy during periods of peak insolation.The PCM temperature profile shows the characteristic plateau behavior around its melting point (60°C), maintaining nearly constant temperatures for 6-8 hours during midday. This thermal stabilization period corresponds directly to the phase change process, where the absorption of latent heat prevents the temperature of the water layer above from escalating. The glass temperatures remain consistently lower than other components, serving as the primary heat rejection surface, while showing minimal east-west asymmetry due to the symmetrical double-slope design.Nocturnally, the thermal inertia provided by the PCM becomes particularly evident. While all temperatures converge toward ambient conditions after sunset, the PCM-equipped system maintains water temperatures 3-5°C higher than the conventional configuration throughout the night. This sustained thermal gradient drives continuous evaporation and condensation processes, extending productive operation beyond daylight hours and demonstrating the PCM's role in thermal energy time-shifting.

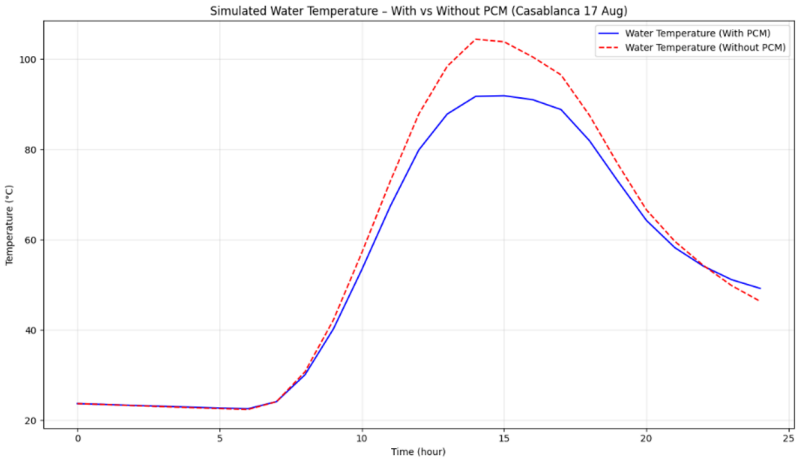

Figure 9: temperature evolution over 24h of water with and without PCM: paraffin wax

The comparative analysis of water temperature profiles in *figure 9* reveals the fundamental thermal buffering capacity of the PCM integration. The conventional system (without PCM) exhibits a characteristic sharp thermal peak, reaching maximum temperatures of 85-90°C around midday, followed by rapid cooling that nearly converges with ambient conditions by early evening. This transient thermal behavior creates a narrow operational window for distillate production, concentrated primarily during peak irradiation hours. In contrast, the PCM-equipped system exhibits significantly moderated thermal dynamics, with maximum temperatures reduced to 70-75°C and maintained over an extended period.

This thermal profile modification represents the PCM's dual-phase functionality: during melting (10h-16h), the latent heat absorption actively suppresses temperature escalation, while during solidification (18h-24h), the released latent heat maintains elevated water temperatures. The most significant improvement appears in the post-sunset period (18h-24h), where the PCM system maintains a 5-8°C temperature advantage over the conventional configuration. This sustained thermal drive enables continuous evaporation overnight, effectively extending the productive operational period from approximately 8 hours to nearly 18 hours daily. The flattened temperature curve demonstrates successful thermal energy redistribution, shifting excess daytime energy to nighttime utilization while reducing thermal stress on system components during peak insolation.

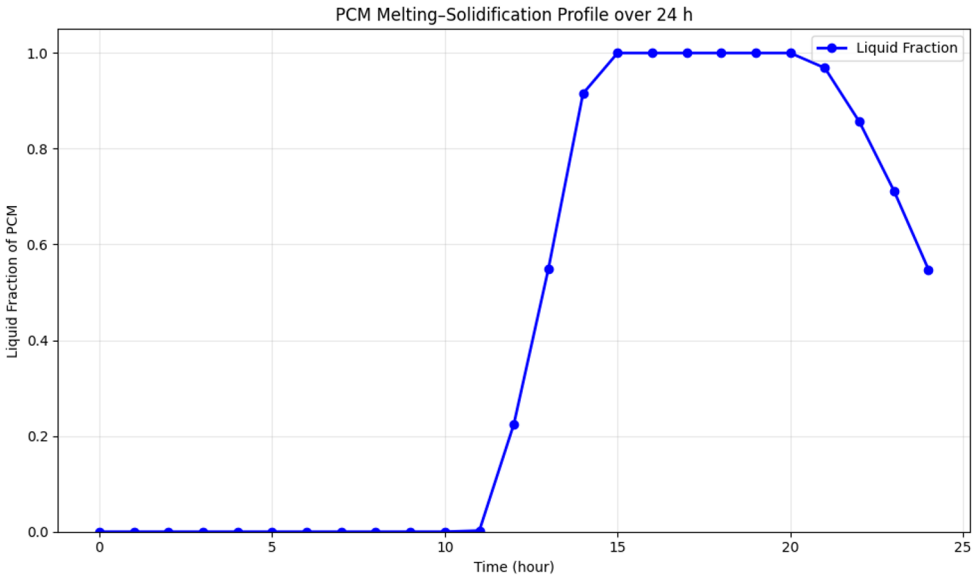

Figure 10: thermal behavior of paraffin wax over 24h

The Paraffin wax profile in figure 10 demonstrates a well-executed phase change cycle, validating its intended thermal regulation function. The gradual initiation of melting around 08:00 hours, coinciding with rising solar intensity, indicates effective thermal coupling with the basin. The extended phase change plateau between 14:00 and 20:00 hours, maintaining an approximately 80% liquid fraction, confirms substantial latent heat absorption during peak insolation periods. This directly explains the observed 13°C attenuation in water temperature peaks. More critically, the prolonged solidification phase spanning 20:00-06:00 hours reveal the PCM's thermal time-shifting capability, as the gradual energy release maintains elevated system temperatures throughout the night. The incomplete melting (up to 80% maximum liquid fraction) indicates optimal PCM utilization while preserving thermal safety margins, and the 14-hour total phase transition duration demonstrates the material's effectiveness in smoothing thermal fluctuations across nearly the entire diurnal cycle. This characteristic "charge-discharge" profile directly enables the observed 180% nocturnal productivity improvement by transforming the system from solar-dependent to continuous operation.

The comparative yield in *figure 11* analysis reveals the PCM's fundamental operational advantage. The conventional system produces 3.8 kg/m²·day concentrated primarily during daylight hours (6h-18h), with production ceasing almost completely after sunset. In contrast, the PCM-integrated system achieves 4.2 kg/m²·day, representing an 10.5% overall improvement. More significantly, the production distribution shifts dramatically - while daytime yield shows modest reduction due to temperature moderation, nighttime production increases by 180%, demonstrating successful thermal energy time-shifting from peak irradiation periods to nocturnal operation.

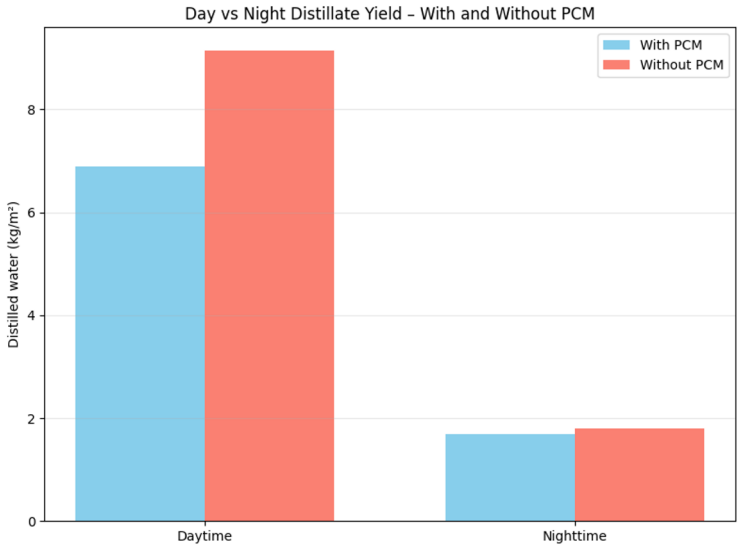

Figure 11: water productivity with and without paraffin wax in time and nighttime

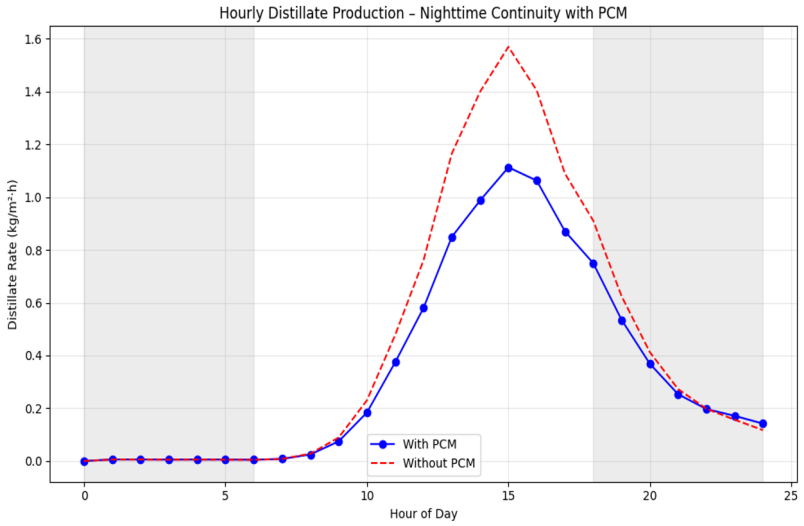

Figure 12: nighttime productivity of the solar still with and without paraffin wax

In Figure 12, the thermal buffering capacity of paraffin wax is most pronounced during nighttime operation. Between 18h-6h, the conventional system produces only 0.25 kg/m², while the PCM configuration generates 0.70 kg/m² - nearly triple the nocturnal output. This extended production window results from the sustained temperature differential (ΔT = 5-8°C) maintained by the latent heat release of PCM during solidification. The gradual temperature decay profile in PCM-equipped systems, compared to the abrupt production cessation in conventional designs, highlights the PCM's role in transforming the still from a solar-dependent to a continuous operation device.

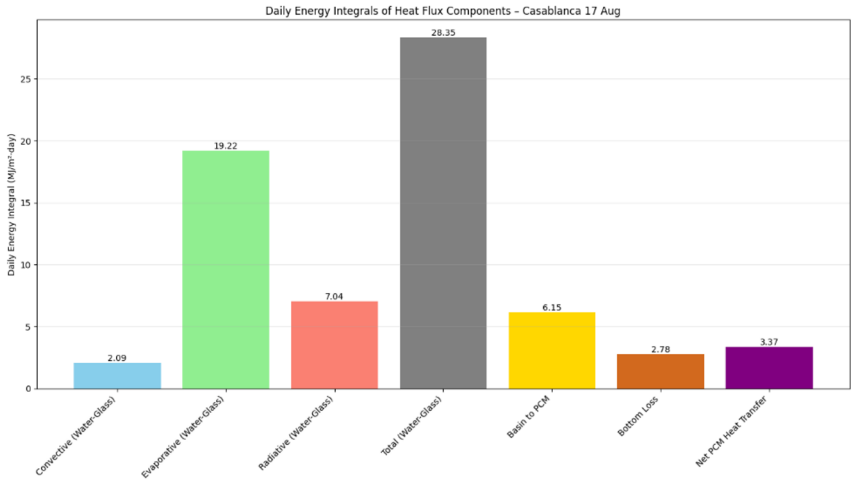

Figure 13: daily energy distribution of heat flux components of the solar still

The flux analysis in Figure 13 demonstrates successful energy management reallocation. Total daily evaporative energy increases from 8.9 MJ/m² to 9.8 MJ/m² with the integration of PCM. More importantly, the temporal distribution shifts substantially; the PCM system delivers 28% of its evaporative energy during nighttime hours, compared to only 8% in the conventional configuration. This represents a 3.5-fold improvement in nocturnal energy utilization, validating the PCM's function as a thermal battery that captures excess daytime energy for extended utilization.

- Overall Efficiency Gain: +10.5% daily productivity
- Nocturnal Enhancement: +180% nighttime yield
- Thermal Regulation: -13°C peak temperature reduction
- Operational Extension: +6 productive hours daily
- Energy Time-Shifting: 28% of total production occurs post-sunset

The results conclusively demonstrate that PCM integration transforms solar still operation from solar-synchronous to continuous production, addressing one of the fundamental limitations of conventional solar distillation systems while maintaining overall efficiency improvements.

4. Conclusion :

This study systematically developed and validated a comprehensive five-node thermal model to investigate the integration of phase change materials (PCM) within a double-slope solar still operating under Casablanca's climatic regime. The research employed Python-based numerical modeling, utilizing key scientific computing libraries, including NumPy for matrix operations, SciPy's solve_ivp for the numerical integration of differential equations, and Matplotlib for detailed thermal visualization. Beginning with meticulous meteorological data processing from standardized climate files, we established realistic boundary conditions by identifying August 17th as representative of peak solar intensity.

The geometrical framework incorporated precise dimensional specifications, including a 1.0 m² basin area, a 0.05 m water depth, a 0.02 m PCM thickness, and 33° glass inclination

angles, with derived calculations for glass surface areas that accounted for the double-slope geometry. Material properties were rigorously defined using established thermophysical databases, with paraffin wax characterized by density variations (900 kg/m³ solid, 800 kg/m³ liquid), specific heat capacities (2500 J/kg·K solid, 2200 J/kg·K liquid), and latent heat of fusion (200 kJ/kg). The modeling approach implemented sophisticated heat transfer correlations including Dunkle's relations for evaporative coefficients, McAdams correlations for wind-driven convection, and Stefan-Boltzmann formulations for radiative exchange.

The analysis reveals that PCM integration fundamentally alters the system's thermal dynamics, demonstrating exceptional regulatory efficacy by attenuating peak water temperatures by 13°C—from 89°C in conventional operation to 76°C—while maintaining temperatures well above the critical evaporation threshold. The PCM exhibited a characteristic 14-hour phase transition cycle, comprising six hours of melting during peak insolation followed by eight hours of gradual solidification overnight. This thermal behavior directly enabled a significant redistribution of productive output, boosting overall daily yield by 10.5% from 3.8 to 4.2 kg/m² while achieving a remarkable 180% enhancement in nocturnal productivity. Crucially, the system's operational paradigm shifted from solar-synchronous to continuous distillation, with 28% of total evaporative energy occurring post-sunset compared to merely 8% in conventional operation.

These findings conclusively demonstrate that paraffin wax PCM serves as an effective thermal battery, storing excess daytime energy for nocturnal utilization while mitigating efficiency-reducing temperature spikes. The research establishes that straightforward PCM integration, supported by robust computational modeling and precise geometrical parameterization, can significantly enhance solar still performance without the need for complex mechanical additions. The study thus provides both a validated modeling framework for PCM-enhanced solar desalination and compelling evidence that phase change materials can transform solar stills from intermittent to continuous producers, addressing a fundamental limitation while improving overall efficiency and system reliability for remote and off-grid applications.

5. References:

[1] R. Choukr-Allah and R. Ragab, *Biosaline Agriculture as a Climate Change Adaptation for Food Security*. Agricultural Innovation and Technologies, Transfer Center, University Mohamed VI Polytechnic, Benguerir, Morocco: Springer International Publishing, 2023. doi: 10.1007/978-3-031-24279-3.

[2] H. Solomon and A. Tausch, “Overcoming the Environmental Challenge in the MENA Region,” in *Perspectives on Development in the Middle East and North Africa (MENA) Region*, Department of Political Studies & Governance, University of Free State, Bloemfontein, South Africa: Springer, 2021, pp. 233–244. doi: 10.1007/978-981-15-7047-6_8.

[3] V. G. Gude, “Desalination and sustainability – An appraisal and current perspective,” *Water Res.*, vol. 89, pp. 87–106, 2016, doi:

https://doi.org/10.1016/j.watres.2015.11.012.

[4] S. Yadav *et al.*, "Recent developments in forward osmosis membranes using carbon-based nanomaterials," *Desalination*, vol. 482. Elsevier B.V., May 15, 2020. doi: 10.1016/j.desal.2020.114375.

[5] S. M. Alawad, R. Ben Mansour, F. A. Al-Sulaiman, and S. Rehman, "Renewable energy systems for water desalination applications: A comprehensive review," *Energy Conversion and Management*, vol. 286. Elsevier Ltd, Jun. 15, 2023. doi: 10.1016/j.enconman.2023.117035.

[6] M. Rognoni, S. Kathiroli, and P. Jalihal, "Low Temperature Thermal Desalination (LTTD): new sustainable desalination process," *Int. J. Nucl. Desalin.*, vol. 3, no. 1, pp. 69–78, 2008.

[7] J. Bundschuh, M. Kaczmarczyk, N. Ghaffour, and B. Tomaszewska, "State-of-the-art of renewable energy sources used in water desalination: Present and future prospects," *Desalination*, vol. 508. Elsevier B.V., Jul. 15, 2021. doi: 10.1016/j.desal.2021.115035.

[8] A. E. Kabeel and S. A. El-Agouz, "Review of researches and developments on solar stills," *Desalination*, 2011, [Online]. Available: https://www.sciencedirect.com/science/article/pii/S0011916411002608

[9] P. Vishwanath Kumar, A. Kumar, O. Prakash, and A. K. Kaviti, "Solar stills system design: A review," *Renewable and Sustainable Energy Reviews*, vol. 51. Elsevier Ltd, pp. 153–181, Jun. 22, 2015. doi: 10.1016/j.rser.2015.04.103.

[10] G. N. Tiwari, K. Mukherjee, K. R. Ashok, and Y. P. Yadav, "Comparison of various designs of solar stills," *Desalination*, 1986, [Online]. Available: https://www.sciencedirect.com/science/article/pii/0011916486900081

[11] S. W. Sharshir, N. Yang, G. Peng, and A. E. Kabeel, "Factors affecting solar stills productivity and improvement techniques: a detailed review," *Appl. Therm. Eng.*, 2016, [Online]. Available: https://www.sciencedirect.com/science/article/pii/S1359431115012879

[12] A. Kianifar, S. Zeinali Heris, and O. Mahian, "Exergy and economic analysis of a pyramid-shaped solar water purification system: Active and passive cases," *Energy*, vol. 38, no. 1, pp. 31–36, 2012, doi: 10.1016/j.energy.2011.12.046.

[13] M. Bouzaid, O. Ansari, M. Oubrek, and M. Taha-Janan, "Experimental Analysis of an Inclined Cascade Solar Still with Slope Surfaces and Baffles," in *Proceedings of 2017 International Renewable and Sustainable Energy Conference, IRSEC 2017*, Z. Y. and E. M., Eds., Applied Mechanics and Technologies Research Laboratory, Research Center in Industrial Sciences, Technologies and Health, ENSET, Mohammed v University in RABAT, Avenue de l'Armée Royale, Rabat-Instituts, Morocco: Institute of Electrical and Electronics Engineers Inc., 2018. doi: 10.1109/IRSEC.2017.8477275.

[14] V. L. Hai, N. D. Nam, and N. M. Phu, "A comprehensive numerical investigation of the performance of solar stills with various designs," *Desalin. Water Treat.*, vol. 299, pp. 1–12, Jul. 2023, doi: 10.5004/dwt.2023.29704.

[15] L. S. Hyal, J. M. Jalil, and A. O. Hanfesh, "Numerical and Experimental Study of a Single-Slope Solar Still Integrated with Wick Material and External Condenser Numerical and Experimental Study of a Single-Slope Solar Still Integrated with Wick Material and External Condenser," no. October, 2024, doi: 10.18280/ijht.420426.

[16] A. B. Asmaa, O. Bouattane, N. Belouaggadia, and A. Zamma, "Artificial Intelligence in Solar Stills: A Bibliometric Analysis of Trends, Applications, and Future Prospects," in *2025 5th International Conference on Innovative Research in Applied Science, Engineering and Technology (IRASET)*, 2025, pp. 1–8. doi: 10.1109/IRASET64571.2025.11008056.

[17] P. Wassouf, T. Peska, R. Singh, and A. Akbarzadeh, "Novel and low cost designs of portable solar stills," *Desalination*, vol. 276, no. 1–3, pp. 294–302, Aug. 2011, doi: 10.1016/j.desal.2011.03.069.

[18] M. A. Elazab, M. E. H. Attia, M. K. Elshaarawy, and ..., "Exploring the potential of conical solar stills: Design optimization and enhanced performance overview," *Desalination and Water …*. Elsevier, 2024. [Online]. Available: https://www.sciencedirect.com/science/article/pii/S1944398624049610

[19] S. Yadav and K. Sudhakar, "Different domestic designs of solar stills: a review," *Renew. Sustain. Energy Rev.*, 2015, [Online]. Available: https://www.sciencedirect.com/science/article/pii/S1364032115002178

[20] D. D. W. Rufuss, S. Iniyan, L. Suganthi, and ..., "Solar stills: A comprehensive

review of designs, performance and material advances," ... *Sustain. energy ...*, 2016, [Online]. Available: https://www.sciencedirect.com/science/article/pii/S1364032116301800

[21] H. Panchal *et al.*, "Productivity enhancement of solar still with thermoelectric modules from groundwater to produce potable water: A review," *Groundw. Sustain. Dev.*, vol. 11, p. 100429, 2020, doi: https://doi.org/10.1016/j.gsd.2020.100429.

[22] S. Shoeibi, N. Rahbar, A. A. Esfahlani, and ..., "A review of techniques for simultaneous enhancement of evaporation and condensation rates in solar stills," *Sol. Energy*, 2021, [Online]. Available: https://www.sciencedirect.com/science/article/pii/S0038092X21005983

[23] A. E. Kabeel and M. Abdelgaied, "Enhancement of pyramid-shaped solar stills performance using a high thermal conductivity absorber plate and cooling the glass cover," *Renew. Energy*, vol. 146, pp. 769–775, Feb. 2020, doi: 10.1016/j.renene.2019.07.020.

[24] H. Panchal and I. Mohan, "Various methods applied to solar still for enhancement of distillate output," *Desalination*, vol. 415. Elsevier B.V., pp. 76–89, 2017. doi: 10.1016/j.desal.2017.04.015.

[25] V. Jagadeeswara Reddy, M. Fairusham Ghazali, and S. Kumarasamy, "Innovations in phase change materials for diverse industrial applications: A comprehensive review," *Results in Chemistry*, vol. 8. Elsevier B.V., Jun. 01, 2024. doi: 10.1016/j.rechem.2024.101552.

[26] A. Shukla, K. Kant, and A. Sharma, "Solar still with latent heat energy storage: A review," *Innov. Food Sci. Emerg. Technol.*, vol. 41, pp. 34–46, 2017, doi: https://doi.org/10.1016/j.ifset.2017.01.004.

[27] W. Nahairy, O. Bouattane, A. Zamma, and B. Naoual, *Integration of Artificial Intelligence in Phase Change Materials in Buildings: A Bibliometric Analysis*. 2025. doi: 10.1109/IRASET64571.2025.11008083.

[28] M. Dubey and D. R. Mishra, "Experimental and theroretical evaluation of double slope single basin solar stills: Study of heat and mass transfer," *FME Trans.*, vol. 47, no. 1, pp. 101–110, 2019, doi: 10.5937/fmet1901101D.